inorganics

MDPI

Article

Stem Bark-Mediated Green Synthesis of Silver Nanoparticles from *Pyrus pashia*: Characterization, Antioxidant, and Antibacterial Properties

Lekha Nath Khanal [1], Purna Prasad Dhakal [2], Mani Ram Kandel [3], Debendra Acharya [4], Ek Raj Baral [5], Kisan Chhetri [4,*] and Surya Kant Kalauni [2,*]

[1] Department of Chemistry, Prithvi Narayan Campus, Tribhuvan University, Pokhara 33700, Nepal; lkhanal7@gmail.com
[2] Central Department of Chemistry, Tribhuvan University, Kathmandu 44613, Nepal; dhakalpurna1@gmail.com
[3] Department of Chemistry, Amrit Campus, Tribhuvan University, Kathmandu 44613, Nepal; mrk.shringa4@gmail.com
[4] Department of Nano Convergence Engineering, Jeonbuk National University, Jeonju 54896, Republic of Korea; debenaracharya88@jbnu.ac.kr
[5] Department of Chemistry, Research Institute of Physics and Chemistry, Jeonbuk National University, Jeonju 54896, Republic of Korea; baralek03@gmail.com
* Correspondence: chhetrikisan88@jbnu.ac.kr (K.C.); skkalauni@gmail.com (S.K.K.)

Abstract: The investigation of using medicinal plants for the production and application of silver nanoparticles (AgNPs) has attracted growing research interest. In this study, AgNPs are synthesized from the stem barks of the *Pyrus pashia* medicinal plant using a biosynthetic strategy. The reaction conditions were optimized under ambient conditions, including concentration, temperature, time, and pH, and various techniques were employed, such as UV-visible, FTIR, XRD, FESEM, and TEM, to characterize the synthesized AgNPs. The AgNPs produced through this biosynthesis method were found to be spherical and polydispersed, with an average size of 23.92 ± 7.04 nm. The synthesized AgNPs demonstrated an enhanced DPPH free radical scavenging capacity compared to the aqueous extract, with IC_{50} values of 10.67 ± 0.05 µg/mL and 13.66 ± 0.35 µg/mL, respectively. In the agar well diffusion method, the synthesized AgNPs showed higher antibacterial activity than that of the extract against *Escherichia coli* (ATCC 25922), *Staphylococcus aureus* (ATCC 25923), *Enterococcus faecalis* (ATCC 29212), *Salmonella typhi* (ATCC 14028), and *Shigella sonnei* (ATCC 25931). Based on these findings, the study suggests that green synthesized AgNPs from *P. pashia* could be used for biomedical applications.

Keywords: green synthesis; *Pyrus pashia*; silver nanoparticles; antioxidant activity; antibacterial activity

Citation: Khanal, L.N.; Dhakal, P.P.; Kandel, M.R.; Acharya, D.; Baral, E.R.; Chhetri, K.; Kalauni, S.K. Stem Bark-Mediated Green Synthesis of Silver Nanoparticles from *Pyrus pashia*: Characterization, Antioxidant, and Antibacterial Properties. *Inorganics* **2023**, *11*, 263. https://doi.org/10.3390/inorganics11060263

Academic Editor: Antonino Gulino

Received: 18 May 2023
Revised: 10 June 2023
Accepted: 19 June 2023
Published: 20 June 2023

1. Introduction

Nanotechnology is one of the exciting fields of research that deals with novel materials of unique properties due to their size, which ranges from 1 to 100 nm [1]. Nanomaterials exhibit entirely different mechanical, thermal, physicochemical, biological, and other properties than their bulk constituents due to their large surface area-to-volume ratio and quantum effect. They have multidimensional applications in the fields of agriculture, biomedical, food, drug delivery, sensing, etc., due to their significant mechanical, catalytic, antimicrobial, antioxidant, optical, and catalytic properties, etc. [2,3]. The nanoparticles of noble metals such as gold, silver, copper, platinum, etc., have drawn attention to biomedical fields due to their multifunctional theragnostic abilities [4]. Nanomaterials are conventionally synthesized by various physical and chemical methods, but they are not safe, cost-effective, or eco-friendly [5]. Due to concerns regarding energy consumption, the practice and release of hazardous chemicals, as well as the complexity of equipment and

synthetic conditions, traditional physical and chemical methods are gradually being replaced by more environmentally friendly approaches, known as green methods. Green materials, such as polyphenols and proteins, can serve as alternatives to chemical reagents for reducing metal ions. By optimizing factors such as the temperature, concentration, pH, and other parameters, the quality of silver nanoparticles (AgNPs) synthesized through green methods can even surpass those produced using physical or chemical methods [6]. Due to their applications in climate change, contamination, antimicrobial activities, information storage, biomedical applications, energy generation, clean water technology, catalysis, biological sensors, optoelectronics, and DNA sequencing, the synthesis of silver nanoparticles has gained a lot of attention [7]. As a result, scientists are involved in safe and green methods to produce nanomaterials by using plants, microbes, biomolecules, etc. These techniques do not practice or exhaust hazardous systems and chemicals in the process [8].

Silver nanoparticles (AgNPs) have attracted the attention of researchers due to their significant antibacterial nature [9]. Metallic silver itself is a safe antibacterial agent at low concentrations because of its oligo-dynamic effect. The presence of toxic silver ions led them to be used as effective antifungal, anti-inflammatory, and antibacterial agents. In recent times, AgNPs have been used in wound dressing, ointments, formulation of dental coatings and bone cement, the lining of food containers, etc., to prevent the growth of drug-resistant microbes [5,10]. Medicinal plants have long been used in traditional medicine for the treatment of several diseases. A large number of bioactive plant secondary metabolites, including alkaloids, flavonoids, steroids, tannins, polyphenols, reducing sugars, glycosides, proteins, vitamins, etc., are the sources of safer medicines or drug-lead compounds. In the synthesis of AgNPs, the phytochemicals serve as reducing, capping, and stabilizing agents to obtain more stable nanoparticles with the desired shape and size. These compounds are easily oxidized by donating hydrogen atoms or electrons to silver ions in solution and converting them into silver atoms. Neutral silver atoms are adsorbed by active functional groups, such as –COOH of glutamine and aspartic acids, and -OH of tyrosine, for the stabilization and growth of polydisperse Ag nanoparticles. The nature and type of the phytoconstituents, pH, temperature, parts used, the concentration of extract/Ag^+ ion, time of reaction, etc., greatly influence the properties of AgNPs [11–13].

Pyrus pashia is a medium-sized deciduous plant of the Rosaceae family distributed in the Himalayan region up to elevations of 2700 m above sea level in Pakistan, India, Nepal, China, and Vietnam. The leaves are simple and ovate, and the flowers are small and white and give rise to small pear-shaped green fruits, which mature from November to December [14]. The leaves, stem barks, flowers, and fruits of the plants have been extensively used in folk medicine, as fodder, and to make healthy beverages. The leaves are astringent, laxative, and febrifuge and have sedative properties. The decoction of leaves and stems is traditionally used for the treatment of sore throat, peptic ulcer, and typhoid fever. Fruits are used as diuretics, astringents, and for the management of eye problems, gastric disorders, abdominal pain, and anemia [15]. The presence of important phytochemicals including alkaloids, polyphenols, flavonoids, terpenoids, tannins, glycosides, reducing sugars, and saponins were reported in the methanol extract of the stem bark of the plant [16].

In this study, AgNPs were fabricated by using the stem barks of the plant that contained the essential compounds required for the synthesis of AgNPs. The parameters affecting the synthesis, such as the pH, concentration, the ratio of the reactants, and the reaction times, were also explored. The synthesized AgNPs were characterized by using UV-visible and Fourier-transform infrared (FTIR) spectroscopy, field emission scanning electron microscopy (FESEM), transmission electron microscopy (TEM), and X-ray diffraction (XRD) analysis. The antioxidant and antibacterial activities of the synthesized AgNPs were evaluated by the 2-2-diphenyl-1-picrylhydrazyl (DPPH) radical scavenging and agar well diffusion methods, respectively.

2. Results and Discussion

2.1. Macro- and Micro-Morphological Analysis

The topology, shape, and size of silver nanoparticles synthesized by using PPAE were analyzed by scanning electron microscopy imaging. The AgNPs were spherical, irregular-shaped, and had quite a disparity in size, which can be seen in the images at different resolutions (Figure 1a–c). The elements in the biosynthesized silver nanoparticles were detected by the energy-dispersive X-ray (EDX) spectrum (Figure 1d–d_3). As shown in Figure 1e, silver was present in the highest quantity (66.75%) at an intense peak at around 3 keV in the EDX spectra, followed by carbon (22.02%) and oxygen (11.23%).

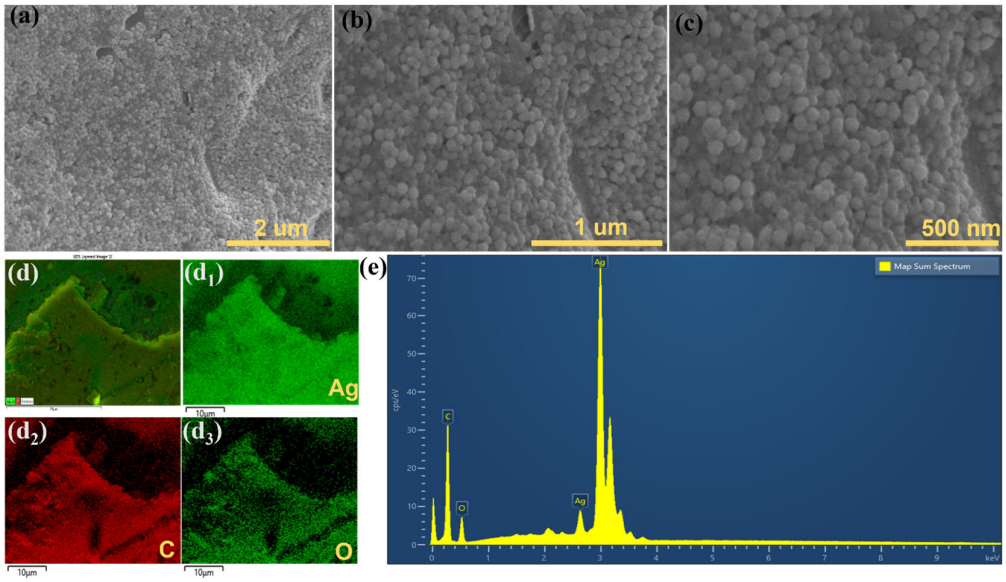

Figure 1. (**a**–**c**) FESEM images of biosynthesized AgNPs, (**d**–**d$_3$**) elemental color mapping of biosynthesized AgNPs, and (**e**) EDX spectrum of biosynthesized AgNPs.

The X-ray diffraction crystallography (XRD) study determines the crystalline nature of the as-synthesized materials [17]. Therefore, the crystalline nature of the silver nanoparticles synthesized using the stem bark extracts of *P. pashia* was confirmed by the XRD analysis. Figure 2a shows clear diffraction peaks at 2θ angles of 38.09°, 44.53°, 64.61°, and 77.50°, corresponding to the crystal planes (111), (200), (220), and (311) of the nanoparticles. The XRD pattern of the synthesized AgNPs is analogous to the face-centered cubic structure of JCPDS file No. 030921 [18]. The same type of crystalline AgNPs were formed in the synthesis by using the leaves of *Millettia pinnata* [19]. Transmission electron microscopy (TEM) is another powerful tool used for determining the morphology and size of metallic nanoparticles. In this study, TEM images revealed the formation of spherical particles with an average size of 23.92 ± 7.04 nm (Figure 2b). The size variation of the synthesized AgNPs from 11.78 to 32.27 nm is shown in the histogram in Figure 2c. The AgNPs synthesized by using different concentrations of *Flos sophorae immaturus* had average sizes of 27.8, 28.5, and 36.5 nm, analogous to our results [20]. Similarly, silver nanoparticles synthesized by using the root barks of *Rubus ellipticus* were spherical and had an average size of 25.20 ± 7.01 nm [21]. The selected area electron diffraction (SAED) pattern of the synthesized silver nanoparticles showed clear concentric rings corresponding to the hkl values of (111), (200), (220), and (311), confirming the FCC crystalline geometry (Figure 2d).

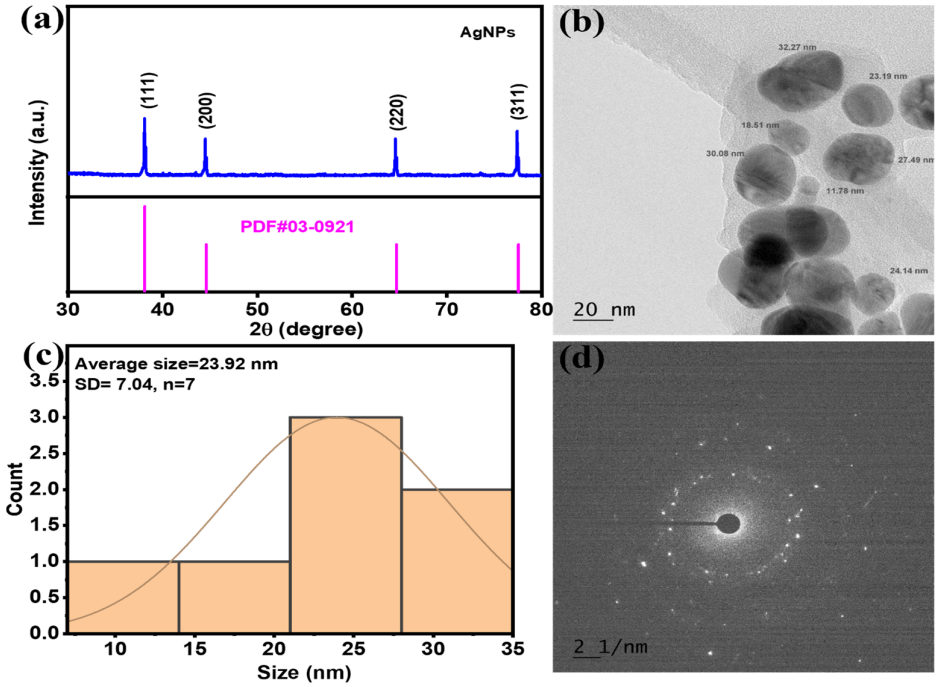

Figure 2. (**a**) XRD pattern of AgNPs synthesized by using PPAE, (**b**) TEM images of AgNPs, (**c**) histogram showing size distribution, and (**d**) SAED pattern of the AgNPs.

2.2. UV-Visible Spectroscopy

The reaction between PPAE and silver nitrate was confirmed by the visual change of color, from the light-yellow color of the extract to reddish brown. The transformation of color is associated with the strong surface plasmon resonance (SPR) phenomenon, which was further confirmed by UV-visible spectroscopy. The surface plasmon resonance of the silver nanoparticles is associated with the interaction of electromagnetic radiation and the electrons in the conduction band around the AgNPs. When the free electrons of metal nanoparticles absorb visible light, they are excited to a higher energy level, and upon returning, they emit light of a particular frequency. The change in optical property is an important parameter that is proportional to the shape and size of the nanoparticles [22]. The highest SPR peak of 0.561 at 436 nm was observed in the reaction mixture containing extract and silver nitrate in the ratio of 1:9, at 25 °C, and the neutral pH indicated an optimized dose for the reaction (Figure 3a). The reaction condition was further tested by changing to pH values of 5.5, 7, 8, and 10 by maintaining the ratio of 1:9 at the same temperature. A narrow peak at 428, with the highest absorption peak for the reaction mixture maintained at a pH of 7, was observed (Figure 3b). The observation of narrow peaks is attributed to the formation of monodispersed and small-sized nanoparticles. There was a very mild and unrecognizable peak at a low peak, but in basic conditions (pH = 10), the formation of nanoparticles was immediate, but precipitation was observed. This might be due to the formation of AgOH and agglomeration. A similar observation of the optimization of the synthesis of silver nanoparticles at a neutral pH of 7 was observed in the synthesis by using the leaf extracts of *Polyalthia longifolia* [23]. In a similar study, the synthesis of silver nanoparticles by using *Terminalia chebula* extract was optimized at a pH of 6.8, with the appearance of a prominent peak in the range of 440 nm on the UV-visible spectra, which is analogous to our observation [24]. Highly stable silver nanoparticles were synthesized by the reaction of 1 mM of $AgNO_3$ with *Acalypha indica* leaf extract. The pH of the reaction was optimized by conducting the reactions at the pH values of 2, 5, 7, 9, 11, and 13. At acidic conditions, synthesis of AgNPs was not reported, while at a higher pH, agglomerations were observed, but no alteration in the peak of the UV-visible spectra at 420 nm was observed even after 2 months. The reaction was instantaneous,

and conversion of the brown color was observed within 30 min of incubation [25]. The formation was proportional to pH up to 8, and then decreased in the synthesis of AgNPs using the aqueous extracts of *Seripheidium quettense*, which was speculated to be due to the ionization of phenolic compounds in the extract.

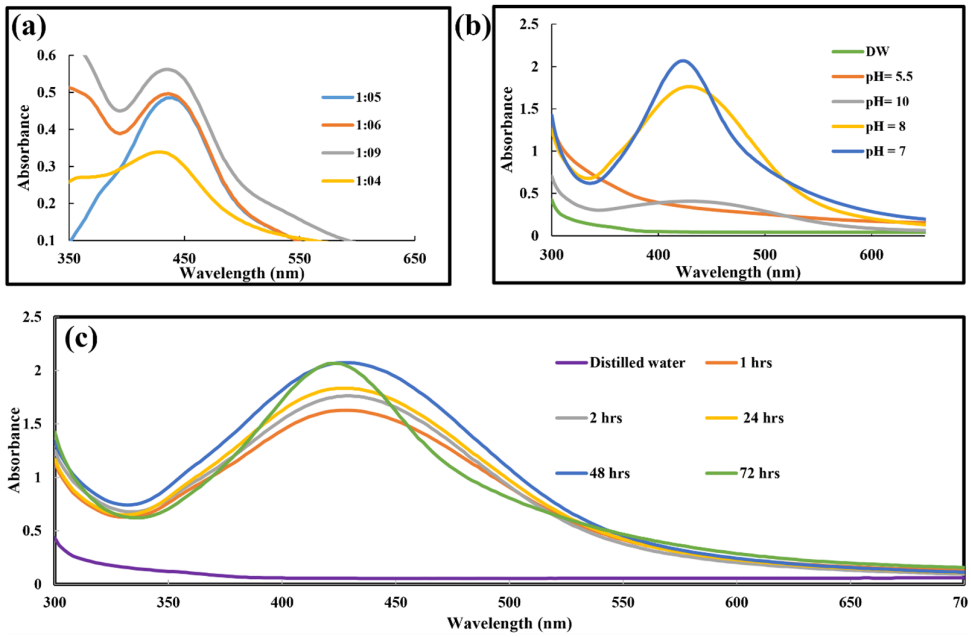

Figure 3. UV-visible spectra of AgNPs (**a**) at different proportions of the reactants (temperature: 25 °C, pH: 7, time = 1 h), (**b**) at different pH ranges of the solutions (temperature: 25 °C, ratio: 1 (extract):9 ($AgNO_3$), time: 1 h), and (**c**) at different times (temperature: 25 °C, ratio: 1 (extract): 9 ($AgNO_3$), pH: 7).

Many literature reports show that acidic pH favors the formation of larger-sized particles, while the higher pH of alkaline conditions favors smaller-sized particles [26]. Although several researchers have reported different optimized conditions for the synthesis, pH 7 is considered an optimal condition for the synthesis at 25–40 °C to obtain spherical and smaller-sized nanoparticles that absorb at lower wavelengths [27]. The UV-visible spectra of the reaction mixture were taken at intervals of 1, 2, 24, 48, and 72 h of the reaction mixture. The intense peaks were obtained at around 428 to 435 nm (Figure 3c). The intensity of the absorption peaks increased with time since more time was available for the reaction to accumulate a higher concentration of AgNPs in the mixture. A narrow peak at a lower wavelength indicates the formation of smaller-sized and broader peaks at higher wavelengths, implying a larger sized and agglomerated AgNPs [28]. The observation of similar peaks in the UV-visible spectroscopy after 48 and 72 h of the reaction indicated the completion of the formation and stability of AgNPs. The observation of peaks at the same position with increased intensities indicated the formation of polydisperse nanoparticles, which is similar to the results of in the synthesis of AgNPs using the extracts of *Sargassum longifolium* [29].

2.3. FTIR Spectroscopy

The existence of functional groups of the nanomaterials can be observed using FTIR spectroscopy. Hence, functional groups in the biomolecules present in the PPAE in the reduction, capping, and stabilization of silver nanoparticles were assessed using this technique. The spectra were taken from 500 to 4000 cm^{-1}, which led to the observation of prominent peaks at different positions, corresponding to the particular functional groups. Certain specific peaks of the PPAE were found to be shifted in the biosynthesized AgNPs (Figure 4).

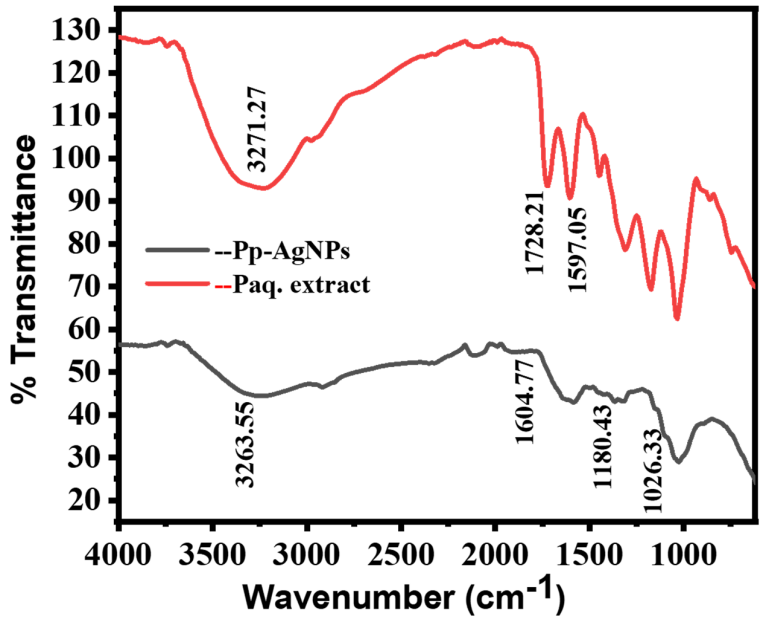

Figure 4. FTIR spectra of AgNPs using PPAE.

A shift towards a lower wavelength at 3271.27 cm^{-1} to 3263.55 cm^{-1} indicates the contribution of the O-H or N-H stretching of phenolics present in the extract [8]. The bands at 1597.05 cm^{-1} and 1604.77 cm^{-1} correspond to C-H stretching, C=O, and C=C bonds in amides of protein molecules in the extract [30]. Other peaks were observed at 1728.21 cm^{-1}, 1180.43 cm^{-1}, and 1026.33 cm^{-1}, due to the presence of carboxylic C=O or ester, (N-H) stretching of amines of proteins, polypeptides, and amino acids [31,32].

2.4. Detection of Phytochemicals in the Extract

The different phytochemicals present in the aqueous stem bark extract of the plant are summarized in Table 1. The results of the phytochemical screening showed the presence of alkaloids, polyphenols, flavonoids, reducing sugars, glycosides, terpenoids, and tannins. These compounds are well-known for their various biological activities, such as antioxidant, antibacterial, anti-inflammatory, antidiabetic, anticancer, etc.

Table 1. Qualitative presence of phytochemicals in PPAE.

S. N.	Phytoconstituents	PPAE
1	Alkaloids	+
2	Polyphenols	++
3	Glycosides	+
4	Reducing sugars	+
5	Terpenoids	++
6	Tannins	++
7	Flavonoids	+

Where (+) = present in trace amounts, (++) = present in abundance.

The polar groups, such as alcohols, phenols, carboxylic acid, amines, etc., present in these molecules reduce and prevent agglomeration, as well as stabilize the silver nanoparticles from silver nitrate solution [8].

2.5. Antioxidant Activity

The in vitro antioxidant capacity of the synthesized silver nanoparticles was evaluated by the DPPH free radical scavenging method, with ascorbic acid as a standard. When the synthesized AgNPs scavenged the free radicals, the color of the DPPH changed to pale yellow. The scavenging capacity of the AgNPs gradually increased with the concentration, that is, proportional to the intensity of color and measured by the absorbance at 517 nm. The dose-dependent variation of the percentage of scavenging capacity with the concentration of the PPAE-synthesized AgNPs and the standard is shown in Figure 5. The graph shows that the synthesized silver nanoparticles had a DPPH free radical scavenging capacity comparable to that of the standard. A similar trend of increase in the scavenging capacity of AgNPs synthesized from *Allium cepa* with concentration was reported by Jini and Sharmila [33]. The half-maximal concentration quenching 50% of the DPPH radical (IC_{50}) value of the synthesized AgNPs (10.67 ± 0.05 µg/mL) was slightly lower than that of its aqueous extract (13.66 ± 0.35 µg/mL) (Table 2).

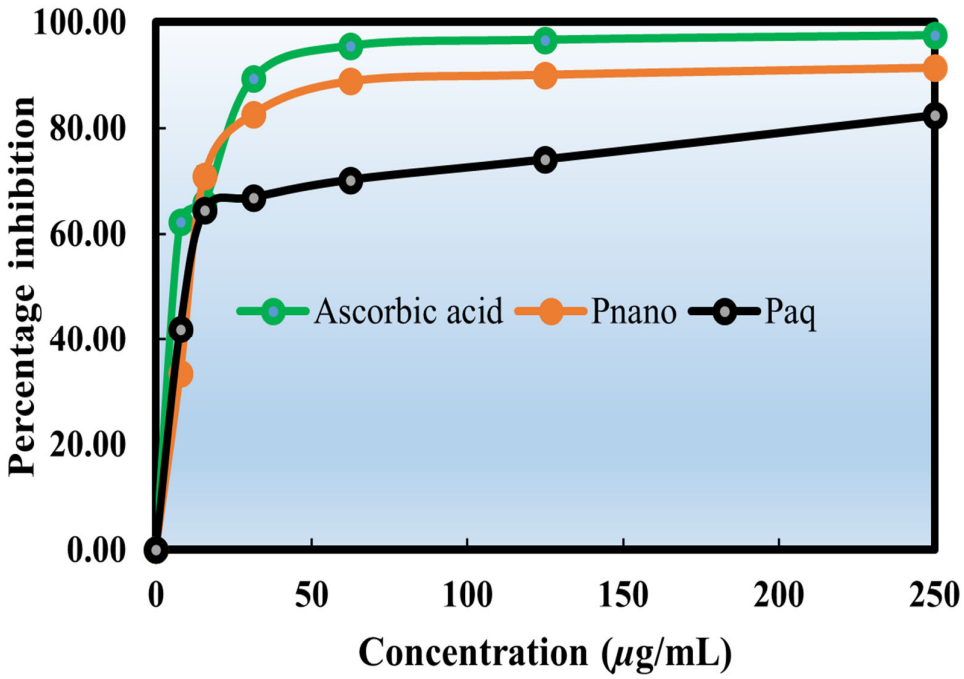

Figure 5. DPPH radical scavenging activity of aqueous extract and Pp-AgNPs.

Table 2. Antioxidant capacity of AgNPs and ascorbic acid.

Samples	IC_{50} (µg/mL)
Ascorbic acid	8.19 ± 0.13
Pp-AgNPs	10.67 ± 0.05
P. pashia (aq.)	13.66 ± 0.35

Where values are the mean ± SD (n = 3).

In our previous work, we reported a slightly higher antioxidant activity (13.85 ± 0.34 µg/mL) of AgNPs synthesized by using root extracts of *Rubus ellipticus*, in comparison to its aqueous extract (IC_{50} = 15.86 ± 4.14 µg/mL) [21]. In a similar study, the AgNPs synthesized by using *Prosopis farcta* fruit extract exhibited a comparable antioxidant activity to that of standard ascorbic acid [34]. The silver nanoparticles synthesized by using the leaf and bark extracts of *Olea ferruginea Royle* also exhibited higher antioxidant activities in comparison to their corresponding crude extracts [35].

Enhanced antioxidant activities of the synthesized AgNPs in comparison to their corresponding crude extracts were reported by Phull et al. by using rhizomes of *Bergenia*

ciliata, and by Dipankar et al. by using the leaf extracts of *Iresine herbstii* [36,37]. Different biomolecules in the plant extract are adsorbed on silver nanoparticles, and the increased surface area of AgNPs allows a greater interaction to neutralize free radicals. A variety of polyphenols, alkaloids, terpenoids, flavonoids, and proteins on the surface of AgNPs donate hydrogen atoms to free radicals and break the chain reactions, as well as catalyze the activities of antioxidant enzymes. Moreover, the unique physicochemical properties of silver nanoparticles, such as the size, shape, surface charge, as well as elemental silver, also contribute to the enhanced antioxidant activity [37]. The free radicals produced in cellular reactions are controlled by the self-antioxidant system of the human body. With increasing age, the concentration of free radicals is not balanced by the body system, leading to oxidative stress. The excess of free radicals in the human body leads to several adverse effects on the biomolecules, such as proteins, DNA, RNA, etc. The deterioration of biomolecules causes cell damage, leading to metabolic disorders and diseases such as Parkinson's disease, Alzheimer's disease, autism, neurodegenerative disorder, and cancer. Antioxidants provided by food supplements either scavenge the free radicals or activate the antioxidative enzymes, to reduce the risk of disease associated with oxidative stress [20].

2.6. Antibacterial Activity

Silver nanoparticles are usually recognized for their strong antibacterial qualities, making them a popular choice for use in various biomedical applications. Their effectiveness comes from their relatively large surface area-to-volume ratio, which allows them to interact more extensively with sulfur- and phosphorus-containing components in bacterial cells, thereby disrupting and killing them [37]. The results of the antibacterial test performed by the agar well diffusion method are shown in Table 3. The test was performed against three Gram-negative and two Gram-positive strains. The results show that for all the bacteria, the activity of the AgNPs was higher than that of the crude extract (Figure 6). The zone of inhibition of *E. coli* (ATCC 25922) increased from 8.5 ± 0.5 mm to 11.5 ± 0.5 mm, *S. aureus* (ATCC 25923) from 7.5 ± 0.5 mm to 11.5 ± 0.5 mm, *E. faecalis* (ATCC 29212) from 6.0 ± 0.0 mm to 9.5 ± 0.5 mm, *S. typhi* (ATCC 14028) from 7.5 ± 0.5 mm to 12.5 ± 0.5 mm, and *S. sonnei* (ATCC 25931) from 8.0 ± 1.0 mm to 12.5 ± 0.5 mm.

Table 3. Antibacterial test results of aqueous extracts and AgNPs.

Samples	Zones of Inhibition (mm)									
	E. coli	**PC**	***S. aureus***	**PC**	***E. faecalis***	**PC**	***S. typhi***	**PC**	***S. sonnei***	**PC**
PPAE	8.5 ± 0.5	18.0	7.5 ± 0.5	15.0	6.0 ± 0.0	12.0	7.5 ± 0.5	18.0	8.0 ± 1.0	18.0
AgNPs	11.5 ± 0.5		11.5 ± 0.5		9.5 ± 0.5		12.5 ± 0.5		12.5 ± 0.5	

Where, PA = *P. pashia* aqueous extract, PN = AgNPs, and PC = positive control. Concentration = 5 mg/mL.

The highest enhancement was observed for *S. typhi.* Similar to our observation, the antibacterial activity of synthesized AgNPs of *Holoptelea integrifolia* leaves against *E. coli* and *S. typhi* was higher than the crude extract [38]. Silver nanoparticles synthesized by using the leaves of *Semecarpus anacardium, Glochidion lanceolarium*, and *Brideia retusa* exhibited enhanced antibacterial and anti-biofilm formation activity against three human pathogens, namely *Pseudomonas aeruginosa, E. coli*, and *S. aureus* [39]. In a separate study, AgNPs synthesized by using aqueous leaf extract of *Cestrum nocturnum* exhibited higher antibacterial activity against *Citrobacter, S. typhi, E. faecalis, E. coli, Proteus vulgaris,* and *Vibrio cholera* on ZOI and MIC measurements. The plant extract was neutral towards all of the bacteria, but the synthesized AgNPs exhibited quite significant activity against all of the tested bacteria [40]. In another study, the AgNPs synthesized by using leaf extract of *Carissa carandas* collected from India also exhibited higher zones of inhibition against *Enterobacter faecalis, Gonococci* spp., *Salmonella typhimurium*, *Citrobacter* spp., and *Shigella flexneri* [41]. Several published papers have reported higher antibacterial activity of AgNPs against Gram-negative bacteria than Gram-positive bacteria.

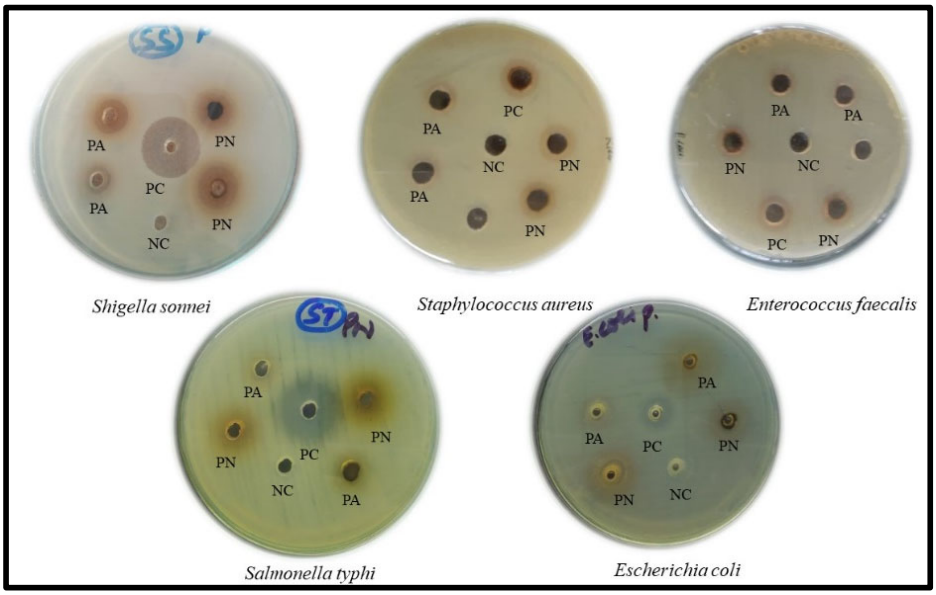

Figure 6. Antibacterial test of PPAE and AgNPs. Note: PA = PPAE, PN = AgNPs, PC = positive control, and NC = negative control.

The authors have explained that the thinner peptidoglycan layer of Gram-negative bacteria was easily penetrated by the AgNPs. Interestingly, in this study, both of the bacteria had similar activities against the AgNPs, which corroborates the observation of the parallel antibacterial activity of AgNPs synthesized by using *Carduus crispus* against *E. coli* and *Micrococcus luteus* [42]. Various accounts have been put forward by several researchers to illustrate the antibacterial mechanism of AgNPs. Wong and Liu describe that the large surface area of AgNPs facilitates contact with bacteria, allowing the nanoparticles to attach to and penetrate the cell membrane [43]. Another possibility is that the nanoparticles or Ag^+ ions interrupt the respiratory chain in the bacteria's mitochondria, ultimately causing cell death. Silver nanoparticles interact with sulfur-containing proteins present in the bacterial membrane and phosphorus-containing components of DNA. When silver nanoparticles enter the bacterial cell, silver ions as well as the AgNPs attack the respiratory chain reactions and inhibit cell division, leading to cell death [44]. This study showed that the antibacterial properties of AgNPs were greater than those of the aqueous extracts. This was likely because the active metabolites present in the extract, such as alkaloids, polyphenols, terpenoids, steroids, and flavonoids, worked together, and might have altered the mechanism. The actual antibacterial mechanism of AgNPs is still a complex and heavily researched topic [7]. The antimicrobial activity of nanoparticles is greatly influenced by various factors, such as size disparity, morphology, shape, and size. Generally, smaller, and monodispersed AgNPs with relatively smaller sizes have been reported to exhibit better biological activities.

They easily enter the cell and interact with the exocyclic nitrogen in the adenine, cytosine, and guanine bases of DNA [45]. The toxicity of silver nanoparticles to mammalian cells and the environment should be properly assessed before the incorporation of many consumer products. The toxicity of AgNPs can be minimized by the prevention of Ag^+, which can easily cross the mammalian cells [7].

Based on the above result and discussion and the further comparison presented in Table 4, *Pyrus pashia* is a prominent medicinal plant and has traditionally been utilized for treating various ailments. Our previous study confirmed the presence of essential phytochemicals, including alkaloids, polyphenols, flavonoids, terpenoids, tannins, glycosides, reducing sugars, and saponins, in the methanol stem bark extract of this plant. Additionally, the extract demonstrated significant antibacterial properties. By utilizing this plant for the synthesis of silver nanoparticles (AgNPs), we aim to not only employ an eco-friendly

method but also tap into Nepal's sustainable resources for biomedical applications. The improvement in antibacterial activity observed in the AgNPs synthesized using this green approach was a significant factor contributing to the selection of *Pyrus pashia* for our study.

Table 4. Comparative table for the synthesis and application of the AgNPS from different parts of plants.

S. No.	Parts of the Plant	Family	Solvents	Shape and Size	Application	References
1.	Leaves of *Citrus sinensis*	Rutaceae	Distilled water (1 mM), $AgNO_3$	Spherical, 78.12 nm	Antioxidant and anticancer	[46]
2.	Leaves of *Murraya koegnigii*	Rutaceae	Distilled water (1 mM), $AgNO_3$	Spherical, anisotropic, 13.54 nm	Antibacterial against MDR bacteria	[47]
3.	Petals of *Hibiscus rosa-sinensis*	Malvaceae	Distilled water (1 mM), $AgNO_3$	Spherical, anisotropic, 76.25 nm	Antibacterial activity against *E. coli*, *S. aureus*, *V. cholera*, and *K. pneumoniae*	[48]
4.	Peels of *Citrus sinensis*	Rutaceae	1 mM $AgNO_3$, nano-cellulose, and hesperidin from orange peel	Spherical and nonuniform, size = 48.11 ± 20.5 nm	Antibacterial against *Xanthomonas axonopodis* pv. *citri* (Xac)	[49]
5.	Leaves of *Pelargonium hortorum* (Geranium)	Geraniaceae	25 mM $AgNO_3$, distilled water, and ethylene glycol	Spherical, anisotropic, size = 35–50 nm	Antifungal against *Candida albicans*	[50]
6.	Rhizome of *Zingiber officinale*	Zingiberaceae	70% ethanol extract + 1 mM $AgNO_3$	Polygonal, heterogenous, size = 20–80 nm	Antimicrobial against *Vibrio anguillarum*, *Vibrioalginolyticus*, *Aeromonas punctata*, *Vibrio parahaemolyticus*, *Vibrio splendidus*, and *Vibrio harveyi*	[51]
7.	Stem barks of *Pongamia pinnata*	Fabaceae	Distilled water, 1 mM $AgNO_3$	Polydispersed, size = 5–55 nm	Antibacterial against *Klebsiella planticola* and *Staphylococcus aureus*	[52]
8.	Stem barks of *Picea abies*	Pinaceae	Distilled water, 1 mM $AgNO_3$/ $AgC_2H_3O_2$	Spherical/ polygonal Size = 44 nm	Antioxidant, and antibacterial against MRSA, *S. aureus*, *K. pneumoniae*, and *Pseudomonasaeruginosa*	[53]

Table 4. *Cont.*

S. No.	Parts of the Plant	Family	Solvents	Shape and Size	Application	References
9.	Seeds of *Coffea arabica*	Rubiaceae	0.1–0.05 M $AgNO_3$ and hydroalcoholic extract	Spherical to ellipsoidal	Antibacterial against *E. coli* and *S. aureus*	[54]
10.	Roots of *Potentilla fulgens*	Rosaceae	Distilled water, 1 mM $AgNO_3$	Spherical size = 10–15 nm	Antibacterial against *E. coli* and *Bacillus subtilis*	[55]
11.	**Stem barks of Pyrus pashia**	**Rosaceae**	**Distilled water, 1 mM $AgNO_3$**	**Spherical size, average diameter = 23.92 nm**	**Antioxidant, and antibacterial against *E.coli*, *S. aureus*, *E. faecalis*, *S. typhi*,and *S. sonnei***	**This Work**

3. Materials and Methods

3.1. Materials

Dimethyl sulfoxide (DMSO; Me_2SO), silver nitrate ($AgNO_3$), and methanol (CH_3OH) were purchased from Thermo Fisher Scientific, India, Pvt. Ltd. The 2,2-diphenyl-1-picrylhydrazyl (DPPH; $C_{18}H_{12}N_5O_6$) was obtained from Tokyo Chemical Industries Co. Ltd., Japan. Muller Hinton Agar (MHA), Muller Hinton Broth (MHB), and neomycin were obtained from Himedia Pvt. Ltd., India. Deionized (DI) water obtained from the Central Department of Chemistry Lab (T.U., Kathmandu, Nepal), and stem bark of *Pyrus pashia* was sampled from Rupa village (Rupa village, Gandaki Province, Nepal). The herbarium of the plant was deposited for botanical authentication (Voucher No. L14; National Herbarium and Plant Laboratories, Godawari, Nepal).

3.2. Preparation and Phytochemical Screening of Plant Extract

Initially, the stem barks were cut into small pieces, washed, and rinsed with DI water. The sample was shade-dried for four weeks and ground into a fine powder using a mechanical mill. Aqueous extract of the plant was prepared by heating 10 g of the sample with 100 mL of DI water in an Erlenmeyer flask of 250 mL capacity. The mixture was carefully heated for about 15 min and filtered through a Whatman No. 1 filter paper. The fresh filtrate of *P. pashia* aqueous extract (PPAE) was used for the synthesis of AgNPs. The qualitative detection of different phytochemicals was performed by adopting standard protocols [56,57]. The test was performed for the presence of alkaloids, flavonoids, polyphenols, terpenoids, reducing sugars, glycosides, and tannins. These secondary metabolites in the PPAE would have a potential role in the reduction of Ag^+ ions and stabilizing the silver nanoparticles.

3.3. Preparation of Silver Nanoparticles

Several parameters, including the concentration of the extract and silver nitrate, temperature, pH, reaction time, etc., play crucial roles in the formation of AgNPs of varying size, shape, and dimension [58]. In this study, we performed the synthesis by varying the concentrations of the reactants, the pH, and the reaction times at lab temperature.

3.4. Effect of Concentration

The reaction was carried out by mixing the plant extract and 1 mM of $AgNO_3$ solution in the ratios of 1:4, 1:5, 1:6, and 1:9, at 25 °C and pH = 7. The aqueous extract of the

plant was dropped into the silver nitrate solution with constant stirring over a magnetic stirrer in the dark. The formation of AgNPs in the solution was indicated by the change of light-yellow to reddish brown color. The reaction mixture was taken after one hour and UV-visible spectra were taken within 300–650 nm. The maximum absorbance observed at 436 nm by the 1:9 reaction mixture indicated the synthesis of AgNPs in the solution.

3.5. Effect of pH

The appearance of the highest peak at 428 nm by the reaction mixture of 1:9 was allowed to react at varying pH values of 5.5, 7, 8, and 10 at the same temperature of 25 °C. The maximum absorbance was observed for the reaction mixture of pH 7.

3.6. Effect of Reaction Time

The reaction between PPAE and the silver nitrate solution was examined at intervals of 1, 2, 24 h, 48 h, and 72 h by UV-visible spectra. The maximum absorbance observed at 48 and 72 h at 430 nm indicated the most favorable condition for the synthesis of the AgNPs.

3.7. Biosynthesis of Silver Nanoparticles (AgNPs)

The optimized conditions were employed for the biosynthesis of silver nanoparticles. A burette was filled with 20 mL of PPAE, and 180 mL of $AgNO_3$ (1 mM) solution was added in a 500 mL conical flask over a magnetic stirrer at room temperature (25 °C). All of the PPAE was carefully dropped into the conical flask, covered with an aluminum foil with constant stirring [32,59]. The change of the light-yellow color into reddish brown within an hour was the visual sign of the development of AgNPs in the solution. After 48 h, the reaction mixture was centrifuged at 8000 rpm for 35 min at 20 °C and successively washed with DI water 3 times. It was collected and centrifuged at 14,000 rpm with double DI water for 35 min. Finally, the solid mass of AgNPs was collected, dehydrated by using ethanol and dried into a desiccator, and stored for characterization and biological studies. Many secondary metabolites such as alkaloids, terpenoids, and steroids with polar groups such as quercetin containing –OH groups reduce silver nitrate into neutral silver atoms (Figure 7). This silver atom is adsorbed by many cyclic peptides and heterocyclic compounds. The capped silver atoms grew into AgNPs of different shapes and sizes depending on various parameters, such as the pH, temperature, reaction time, and concentration [60].

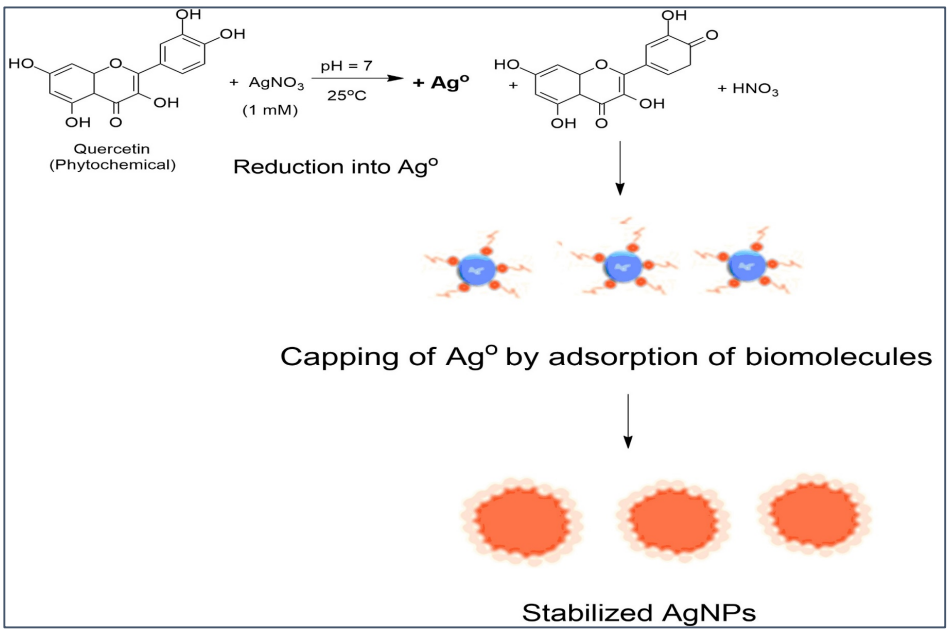

Figure 7. Molecular mechanism of the synthesis and stabilization of AgNPs.

3.8. Characterization of Silver Nanoparticles

The reduction of silver nitrate solution was monitored by visual observation of the color change and UV-visible spectra taken at various intervals of time. The reaction mixture was diluted with DI water and the spectra were taken using the Bio Tek Synergy LX multimode reader at the intervals of 1, 2, 24, 48, and 72 h of the reaction. The functional groups that have a potential role in the reduction, capping, and stabilization of silver nanoparticles were identified by the comparative observation of the FTIR spectra of PPAE and the synthesized AgNPs. The spectra were taken by a Shimadzu IRTracer-100 from 4000 to 400 cm^{-1}. The crystallinity of the silver nanoparticles was confirmed by taking the diffractogram using an X-ray diffractometer (Rigaku Co., Japan). The diffractogram was taken through a dried layer of the sample over the sample holder by using a current of 30 mA, and a voltage of 40 kV with radiation of CuKα (λ = 1.5406 Å), with the scan rate of 10° per minute across the 2θ angle from 0 to 90°. The FESEM images were taken using the Hitachi S-7400 (Japan), equipped with EDX. The TEM images and selected area electron diffraction (SAED) pattern were taken by a JEM-2100 plus at 200 kV (JEOL Ltd., Japan). The suspension of the sample was layered onto the copper tape coated with carbon and mounted in the sample holder of the microscopes. The sizes of the AgNPs were measured from the TEM images by using ImageJ software.

3.9. In Vitro Antioxidant Activity

The antioxidant capacity of the biosynthesized AgNPs was assessed by the DPPH free radical scavenging method, using ascorbic acid as a standard [61,62]. The synthesized AgNPs were dissolved in 50% DMSO and diluted to different concentrations by serial dilution. Each of the solutions were mixed with 0.1 mM of DPPH solution (100:100 µL) in the bores of a 96-well plate, in triplicates. The mixtures were incubated in the dark for 30 min at lab temperature. Then, optical density was measured by using a microplate reader at 517 nm against the blank. The percentage of scavenging of all the test solutions and the standard was calculated by using the formula:

$$\text{Percentage scavenging} = \frac{\text{A(blank)} - \text{A(sample)}}{\text{A(blank)}} \times 100 \quad (1)$$

where A (blank) = absorbance of the blank, and A (sample) = absorbance of the test solutions.

The dose-dependent variation of the DPPH free radical scavenging capacity of the synthesized AgNPs was compared with ascorbic acid. The concentration of AgNPs that inhibited 50% of the DPPH radical (IC_{50}) was calculated by using the GraphPad Prism 9 software.

3.10. Antibacterial Activity

The antibacterial susceptibility of the green synthesized silver nanoparticles was evaluated by the agar well diffusion method [63,64]. The test was performed against both Gram-negative and Gram-positive bacteria (Table 5). The bacteria were cultured into the fresh Muller Hinton Broth (MHB) solution overnight at 37 °C to equalize the turbidity to that of 0.5 McFarland's standard. The suspension was uniformly coated onto the surface of sterile Muller Hinton Agar (MHA) discs with sterile cotton swabs. Using a sterile cork-borer, 6 mm-diameter wells were punched on the MHA plates at equal spaces. The wells were filled with 50 µL of the AgNPs (1 mg/mL) in duplicates, along with a blank and neomycin as a positive control, and incubated for one day at 37 °C. On the next day, the discs were taken out, and the clear circles around the sample holes corresponding to the specific inhibition zones were measured and recorded.

Table 5. List of bacteria used in the study.

S. No.	Name of Bacteria	ATCC	Type
1	*Escherichia coli*	25922	Gram-negative
2	*Staphylococcus aureus*	25923	Gram-positive
3	*Enterococcus faecalis*	29212	Gram-positive
4	*Salmonella typhi*	14028	Gram-negative
5	*Shigella sonnei*	25931	Gram-negative

3.11. Statistical Analysis

The experiments for the antibacterial tests were performed in duplicates and the results were expressed as mean ± SD. The optical density of the DPPH test was processed by Gen5 Microplate Data Collection and Analysis and Microsoft Excel. The tests were performed in triplicates, and the half-maximal concentrations (IC_{50}) were calculated by the GraphPad Prism 9 software.

4. Conclusions

This study successfully developed a rapid and environmentally friendly method to synthesize silver nanoparticles (AgNPs) using the stem bark extracts of *P. pashia*. The AgNPs produced were stable, well-dispersed, and highly pure. This plant extract-mediated synthesis of AgNPs offers a promising alternative to conventional chemical processes, which can be harmful to the environment and health due to their toxic nature. By utilizing plant extracts as reducing agents and stabilizers, this green synthesis technique can be easily scaled up for large-scale production, making it an eco-friendly approach with wide applicability. The synthesized AgNPs had a face-centered crystalline nature with an average size of 23.92 ± 7.04 nm. The green synthesized AgNPs exhibited an enhanced antioxidant activity (IC_{50} = 10.67 ± 0.05 µg/mL) compared to the crude extract (IC_{50} = 13.66 ± 0.35 µg/mL). The antibacterial susceptibility of the synthesized silver nanoparticles was also higher than that of the plant extract. Moreover, the antibacterial test performed by the agar well diffusion method revealed that the AgNPs had similar activities against both the Gram-negative and Gram-positive bacteria. The study emphasizes the need for additional exploration into the potential use of plant extracts in the eco-friendly production of various metallic nanoparticles. Further studies would involve optimizing the process to enhance its effectiveness and assess its toxicity for use in different biomedical applications.

Author Contributions: L.N.K.: conceptualization, methodology, investigation, formal analysis, validation, writing—original draft; P.P.D.: methodology, data curation, visualization; M.R.K.: methodology, data curation, visualization; D.A.: methodology, data curation, visualization; E.R.B.: methodology, data curation, visualization; K.C.: conceptualization, data curation, writing—review and editing, supervision; S.K.K.: conceptualization, writing—original draft, writing—review and editing, supervision, project administration. All authors have read and agreed to the published version of the manuscript.

Funding: This research received no external funding.

Data Availability Statement: Data will be made available upon request.

Conflicts of Interest: The authors declare that they have no known competing financial interests or personal relationships that could have appeared to influence the work reported in this paper.

References

1. Rafique, M.; Sadaf, I.; Rafique, M.S.; Tahir, M.B. A Review on Green Synthesis of Silver Nanoparticles and Their Applications. *Artif. Cells Nanomed. Biotechnol.* **2017**, *45*, 1272–1291. [CrossRef]
2. Hawar, S.N.; Al-Shmgani, H.S.; Al-Kubaisi, Z.A.; Sulaiman, G.M.; Dewir, Y.H.; Rikisahedew, J.J. Green Synthesis of Silver Nanoparticles from *Alhagi graecorum* Leaf Extract and Evaluation of Their Cytotoxicity and Antifungal Activity. *J. Nanomater.* **2022**, *2022*, 1058119. [CrossRef]

3. Shrestha, D.; Nayaju, T.; Kandel, M.R.; Pradhananga, R.R.; Park, C.H.; Kim, C.S. Rice Husk-Derived Mesoporous Biogenic Silica Nanoparticles for Gravity Chromatography. *Heliyon* **2023**, *9*, e15142. [CrossRef]
4. Abdel-Raouf, N.; Al-Enazi, N.M.; Ibraheem, I.B.M.; Alharbi, R.M.; Alkhulaifi, M.M. Biosynthesis of Silver Nanoparticles by Using of the Marine Brown Alga *Padina pavonia* and Their Characterization. *Saudi J. Biol. Sci.* **2019**, *26*, 1207–1215. [CrossRef]
5. Adhikari, A.; Chhetri, K.; Acharya, D.; Pant, B.; Adhikari, A. Green Synthesis of Iron Oxide Nanoparticles Using *Psidium guajava* L. Leaves Extract for Degradation of Organic Dyes and Anti-Microbial Applications. *Catalysts* **2022**, *12*, 1188. [CrossRef]
6. Ying, S.; Guan, Z.; Ofoegbu, P.C.; Clubb, P.; Rico, C.; He, F.; Hong, J. Green Synthesis of Nanoparticles: Current Developments and Limitations. *Environ. Technol. Innov.* **2022**, *26*, 102336. [CrossRef]
7. Vanlalveni, C.; Lallianrawna, S.; Biswas, A.; Selvaraj, M.; Changmai, B.; Rokhum, S.L. Green Synthesis of Silver Nanoparticles Using Plant Extracts and Their Antimicrobial Activities: A Review of Recent Literature. *RSC Adv.* **2021**, *11*, 2804–2837. [CrossRef] [PubMed]
8. Hemlata; Meena, P.R.; Singh, A.P.; Tejavath, K.K. Biosynthesis of Silver Nanoparticles Using *Cucumis prophetarum* Aqueous Leaf Extract and Their Antibacterial and Antiproliferative Activity against Cancer Cell Lines. *ACS Omega* **2020**, *5*, 5520–5528. [CrossRef]
9. Adhikari, A.; Lamichhane, L.; Adhikari, A.; Gyawali, G.; Acharya, D.; Baral, E.R.; Chhetri, K. Green Synthesis of Silver Nanoparticles Using *Artemisia vulgaris* Extract and Its Application toward Catalytic and Metal-Sensing Activity. *Inorganics* **2022**, *10*, 113. [CrossRef]
10. Mohamed, D.S.; El-Baky, R.M.A.; Sandle, T.; Mandour, S.A.; Ahmed, E.F. Antimicrobial Activity of Silver-Treated Bacteria against Other Multi-Drug Resistant Pathogens in Their Environment. *Antibiotics* **2020**, *9*, 181. [CrossRef] [PubMed]
11. Jain, N.; Jain, P.; Rajput, D.; Patil, U.K. Green Synthesized Plant-Based Silver Nanoparticles: Therapeutic Prospective for Anticancer and Antiviral Activity. *Micro Nano Syst. Lett.* **2021**, *9*, 5. [CrossRef]
12. Sharma, V.; Kaushik, S.; Pandit, P.; Dhull, D.; Yadav, J.P.; Kaushik, S. Green Synthesis of Silver Nanoparticles from Medicinal Plants and Evaluation of Their Antiviral Potential against *Chikungunya virus*. *Appl. Microbiol. Biotechnol.* **2019**, *103*, 881–891. [CrossRef]
13. Rahuman, H.B.H.; Dhandapani, R.; Narayanan, S.; Palanivel, V.; Paramasivam, R.; Subbarayalu, R.; Thangavelu, S.; Muthupandian, S. Medicinal Plants Mediated the Green Synthesis of Silver Nanoparticles and Their Biomedical Applications. *IET Nanobiotechnol.* **2022**, *16*, 115–144. [CrossRef] [PubMed]
14. Prakash, O.; Selvi, M.K.; Vijayaraj, P.; Kudachikar, V.B. Lipidome, Nutraceuticals and Nutritional Profiling of *Pyrus pashia* Buch.-Ham Ex D. Don (Kainth) Seeds Oil and Its Antioxidant Potential. *Food Chem.* **2021**, *338*, 128067. [CrossRef] [PubMed]
15. Janbaz, K.H.; Ahsan, M.Z.; Saqib, F.; Imran, I.; Zia-Ul-Haq, M.; Rashid, M.A.; Jaafar, H.Z.E.; Moga, M. Scientific Basis for Use of *Pyrus pashia* Buch.-Ham. Ex D. Don. Fruit in Gastrointestinal, Respiratory and Cardiovascular Ailments. *PLoS ONE* **2015**, *10*, e0118605. [CrossRef]
16. Khanal, L.N.; Sharma, K.R.; Pokharel, Y.R.; Kalauni, S.K. Assessment of Phytochemical, Antioxidant and Antimicrobial Activities of Some Medicinal Plants from Kaski District of Nepal. *Am. J. Plant Sci.* **2020**, *11*, 1383–1397. [CrossRef]
17. Kandel, M.R.; Pan, U.N.; Dhakal, P.P.; Ghising, R.B.; Nguyen, T.T.; Zhao, J.; Kim, N.H.; Lee, J.H. Unique Heterointerface Engineering of Ni_2P-MnP Nanosheets Coupled Co_2P Nanoflowers as Hierarchical Dual-Functional Electrocatalyst for Highly Proficient Overall Water-Splitting. *Appl. Catal. B Environ.* **2023**, *331*, 122680. [CrossRef]
18. Balaji, D.S.; Basavaraja, S.; Deshpande, R.; Mahesh, D.B.; Prabhakar, B.K.; Venkataraman, A. Extracellular Biosynthesis of Functionalized Silver Nanoparticles by Strains of *Cladosporium cladosporioides* Fungus. *Colloids Surf. B Biointerfaces* **2009**, *68*, 88–92. [CrossRef]
19. Rajakumar, G.; Gomathi, T.; Thiruvengadam, M.; Rajeswari, V.D.; Kalpana, V.N.; Chung, I.-M. Evaluation of anti-cholinesterase, antibacterial and cytotoxic activities of green synthesized silver nanoparticles using from *Millettia pinnata* flower extract. *Microb. Pathog.* **2017**, *103*, 123–128. [CrossRef]
20. Cheng, Z.; Tang, S.W.; Feng, J.; Wu, Y. Biosynthesis and Antibacterial Activity of Silver Nanoparticles Using *Flos Sophorae Immaturus* Extract. *Heliyon* **2022**, *8*, e10010. [CrossRef]
21. Khanal, L.N.; Sharma, K.R.; Paudyal, H.; Parajuli, K.; Dahal, B.; GC, G.; Pokharel, Y.R.; Kalauni, S.K. Green Synthesis of Silver Nanoparticles from Root Extracts of *Rubus ellipticus* Sm. and Comparison of Antioxidant and Antibacterial Activity. *J. Nanomater.* **2022**, *2022*, 1832587. [CrossRef]
22. Behravan, M.; Panahi, A.H.; Naghizadeh, A.; Ziaee, M.; Mahdavi, R.; Mirzapour, A. Facile Green Synthesis of Silver Nanoparticles Using *Berberis vulgaris* Leaf and Root Aqueous Extract and Its Antibacterial Activity. *Int. J. Biol. Macromol.* **2019**, *124*, 148–154. [CrossRef] [PubMed]
23. Dashora, A.; Rathore, K.; Raj, S.; Sharma, K. Synthesis of Silver Nanoparticles Employing *Polyalthia longifolia* Leaf Extract and Their In Vitro Antifungal Activity against Phytopathogen. *Biochem. Biophys. Rep.* **2022**, *31*, 101320. [CrossRef]
24. Edison, T.J.I.; Sethuraman, M.G. Instant Green Synthesis of Silver Nanoparticles Using *Terminalia chebula* Fruit Extract and Evaluation of Their Catalytic Activity on Reduction of Methylene Blue. *Process Biochem.* **2012**, *47*, 1351–1357. [CrossRef]
25. Krishnaraj, C.; Ramachandran, R.; Mohan, K.; Kalaichelvan, P.T. Optimization for Rapid Synthesis of Silver Nanoparticles and Its Effect on *Phytopathogenic fungi*. *Spectrochim. Acta Part A Mol. Biomol. Spectrosc.* **2012**, *93*, 95–99. [CrossRef]

26. Nasar, M.Q.; Zohra, T.; Khalil, A.T.; Saqib, S.; Ayaz, M.; Ahmad, A.; Shinwari, Z.K. *Seripheidium quettense* Mediated Green Synthesis of Biogenic Silver Nanoparticles and Their Theranostic Applications. *Green Chem. Lett. Rev.* **2019**, *12*, 310–322. [CrossRef]
27. Ovais, M.; Khalil, A.T.; Raza, A.; Khan, M.A.; Ahmad, I.; Islam, N.U.; Saravanan, M.; Ubaid, M.F.; Ali, M.; Shinwari, Z.K. Green Synthesis of Silver Nanoparticles via Plant Extracts: Beginning a New Era in Cancer Theranostics. *Nanomedicine* **2016**, *12*, 3157–3177. [CrossRef] [PubMed]
28. Smitha, S.L.; Nissamudeen, K.M.; Philip, D.; Gopchandran, K.G. Studies on Surface Plasmon Resonance and Photoluminescence of Silver Nanoparticles. *Spectrochim. Acta Part A Mol. Biomol. Spectrosc.* **2008**, *71*, 186–190. [CrossRef] [PubMed]
29. Rajeshkumar, S.; Malarkodi, C.; Paulkumar, K.; Vanaja, M.; Gnanajobitha, G.; Annadurai, G. Algae Mediated Green Fabrication of Silver Nanoparticles and Examination of Its Antifungal Activity against Clinical Pathogens. *Int. J. Met.* **2014**, *2014*, 692643. [CrossRef]
30. Rosman, N.S.R.; Harun, N.A.; Idris, I.; Ismail, W.I.W. Eco-Friendly Silver Nanoparticles (AgNPs) Fabricated by Green Synthesis Using the Crude Extract of Marine Polychaete, *Marphysa moribidii*: Biosynthesis, Characterisation, and Antibacterial Applications. *Heliyon* **2020**, *6*, e05462. [CrossRef]
31. Afreen, A.; Ahmed, R.; Mehboob, S.; Tariq, M.; Alghamdi, H.A.; Zahid, A.A.; Ali, I.; Malik, K.; Hasan, A. Phytochemical-Assisted Biosynthesis of Silver Nanoparticles from *Ajuga bracteosa* for Biomedical Applications. *Mater. Res. Express* **2020**, *7*, 075404. [CrossRef]
32. Rautela, A.; Rani, J.; Debnath (Das), M. Green Synthesis of Silver Nanoparticles from Tectona Grandis Seeds Extract: Characterization and Mechanism of Antimicrobial Action on Different Microorganisms. *J. Anal. Sci. Technol.* **2019**, *10*, 5. [CrossRef]
33. Jini, D.; Sharmila, S. Green Synthesis of Silver Nanoparticles from *Allium cepa* and Its In Vitro Antidiabetic Activity. *Mater. Today Proc.* **2020**, *22*, 432–438. [CrossRef]
34. Salari, S.; Bahabadi, S.E.; Samzadeh-Kermani, A.; Yosefzaei, F. In-Vitro Evaluation of Antioxidant and Antibacterial Potential of Green Synthesized Silver Nanoparticles Using *Prosopis farcta* Fruit Extract. *Iran. J. Pharm. Res.* **2018**, *18*, 430–445.
35. Hussain, A.; Mehmood, A.; Murtaza, G.; Ahmad, K.S.; Ulfat, A.; Khan, M.F.; Ullah, T.S. Environmentally Benevolent Synthesis and Characterization of Silver Nanoparticles Using *Olea ferruginea* Royle for Antibacterial and Antioxidant Activities. *Green Process. Synth.* **2020**, *9*, 451–461. [CrossRef]
36. Phull, A.-R.; Abbas, Q.; Ali, A.; Raza, H.; Kim, S.J.; Zia, M.; Haq, I. Antioxidant, Cytotoxic and Antimicrobial Activities of Green Synthesized Silver Nanoparticles from Crude Extract of Bergenia Ciliata. *Future J. Pharm. Sci.* **2016**, *2*, 31–36. [CrossRef]
37. Dipankar, C.; Murugan, S. The Green Synthesis, Characterization and Evaluation of the Biological Activities of Silver Nanoparticles Synthesized from *Iresine herbstii* Leaf Aqueous Extracts. *Colloids Surf. B Biointerfaces* **2012**, *98*, 112–119. [CrossRef]
38. Kumar, V.; Singh, S.; Srivastava, B.; Bhadouria, R.; Singh, R. Green Synthesis of Silver Nanoparticles Using Leaf Extract of *Holoptelea integrifolia* and Preliminary Investigation of Its Antioxidant, Anti-Inflammatory, Antidiabetic and Antibacterial Activities. *J. Environ. Chem. Eng.* **2019**, *7*, 103094. [CrossRef]
39. Mohanta, Y.K.; Biswas, K.; Jena, S.K.; Hashem, A.; Allah, E.F.A.; Mohanta, T.K. Anti-Biofilm and Antibacterial Activities of Silver Nanoparticles Synthesized by the Reducing Activity of Phytoconstituents Present in the Indian Medicinal Plants. *Front. Microbiol.* **2020**, *11*, 1143. [CrossRef]
40. Keshari, A.K.; Srivastava, R.; Singh, P.; Yadav, V.B.; Nath, G. Antioxidant and Antibacterial Activity of Silver Nanoparticles Synthesized by *Cestrum nocturnum*. *J. Ayurveda Integr. Med.* **2020**, *11*, 37–44. [CrossRef]
41. Singh, R.; Hano, C.; Nath, G.; Sharma, B. Green Biosynthesis of Silver Nanoparticles Using Leaf Extract of *Carissa carandas* L. and Their Antioxidant and Antimicrobial Activity against Human Pathogenic Bacteria. *Biomolecules* **2021**, *11*, 299. [CrossRef] [PubMed]
42. Urnukhsaikhan, E.; Bold, B.-E.; Gunbileg, A.; Sukhbaatar, N.; Mishig-Ochir, T. Antibacterial Activity and Characteristics of Silver Nanoparticles Biosynthesized from *Carduus crispus*. *Sci. Rep.* **2021**, *11*, 21047. [CrossRef]
43. Wong, K.K.Y.; Liu, X. Silver Nanoparticles—The Real "Silver Bullet" in Clinical Medicine? *Medchemcomm* **2010**, *1*, 125–131. [CrossRef]
44. Rai, M.; Yadav, A.; Gade, A. Silver Nanoparticles as a New Generation of Antimicrobials. *Biotechnol. Adv.* **2009**, *27*, 76–83. [CrossRef] [PubMed]
45. Durán, N.; Durán, M.; de Jesus, M.B.; Seabra, A.B.; Fávaro, W.J.; Nakazato, G. Silver Nanoparticles: A New View on Mechanistic Aspects on Antimicrobial Activity. *Nanomed. Nanotechnol. Biol. Med.* **2016**, *12*, 789–799. [CrossRef]
46. Chen, F.; Zheng, Q.; Li, X.; Xiong, J. *Citrus sinensis* Leaf Aqueous Extract Green-Synthesized Silver Nanoparticles: Characterization and Cytotoxicity, Antioxidant, and Anti-Human Lung Carcinoma Effects. *Arab. J. Chem.* **2022**, *15*, 103845. [CrossRef]
47. Qais, F.A.; Shafiq, A.; Khan, H.M.; Husain, F.M.; Khan, R.A.; Alenazi, B.; Alsalme, A.; Ahmad, I. Antibacterial Effect of Silver Nanoparticles Synthesized Using *Murraya koenigii* (L.) against Multidrug-Resistant Pathogens. *Bioinorg. Chem. Appl.* **2019**, *2019*, 4649506. [CrossRef]
48. Nayak, D.; Ashe, S.; Rauta, P.R.; Nayak, B. Biosynthesis, Characterisation and Antimicrobial Activity of Silver Nanoparticles Using *Hibiscus rosa-sinensis* Petals Extracts. *IET nanobiotechnol.* **2015**, *9*, 288–293. [CrossRef]
49. de Barros, C.H.N.; Cruz, G.C.F.; Mayrink, W.; Tasic, L. Bio-Based Synthesis of Silver Nanoparticles from Orange Waste: Effects of Distinct Biomolecule Coatings on Size, Morphology, and Antimicrobial Activity. *Nanotechnol. Sci. Appl.* **2018**, *11*, 1–14. [CrossRef]

50. Serrano-Díaz, P.; Williams, D.W.; Vega-Arreguin, J.; Manisekaran, R.; Twigg, J.; Morse, D.; García-Contreras, R.; Arenas-Arrocena, M.C.; Acosta-Torres, L.S. *Geranium* Leaf-Mediated Synthesis of Silver Nanoparticles and Their Transcriptomic Effects on Candida Albicans. *Green Process. Synth.* **2023**, *12*, 20228105. [CrossRef]
51. Yang, N.; Li, F.; Jian, T.; Liu, C.; Sun, H.; Wang, L.; Xu, H. Biogenic Synthesis of Silver Nanoparticles Using Ginger (*Zingiber officinale*) Extract and Their Antibacterial Properties against Aquatic Pathogens. *Acta Oceanol. Sin.* **2017**, *36*, 95–100. [CrossRef]
52. Rajeshkumar, S. Synthesis of Silver Nanoparticles Using Fresh Bark of *Pongamia pinnata* and Characterization of Its Antibacterial Activity against Gram Positive and Gram Negative Pathogens. *Resour. Technol.* **2016**, *2*, 30–35. [CrossRef]
53. Tanase, C.; Berta, L.; Coman, N.A.; Roşca, I.; Man, A.; Toma, F.; Mocan, A.; Nicolescu, A.; Jakab-Farkas, L.; Biró, D.; et al. Antibacterial and Antioxidant Potential of Silver Nanoparticles Biosynthesized Using the Spruce Bark Extract. *Nanomaterials* **2019**, *9*, 1541. [CrossRef] [PubMed]
54. Dhand, V.; Soumya, L.; Bharadwaj, S.; Chakra, S.; Bhatt, D.; Sreedhar, B. Green Synthesis of Silver Nanoparticles Using *Coffea arabica* Seed Extract and Its Antibacterial Activity. *Mater. Sci. Eng. C* **2016**, *58*, 36–43. [CrossRef] [PubMed]
55. Mittal, A.K.; Tripathy, D.; Choudhary, A.; Aili, P.K.; Chatterjee, A.; Singh, I.P.; Banerjee, U.C. Bio-Synthesis of Silver Nanoparticles Using *Potentilla fulgens* Wall. Ex Hook. and Its Therapeutic Evaluation as Anticancer and Antimicrobial Agent. *Mater. Sci. Eng. C* **2015**, *53*, 120–127. [CrossRef]
56. Hui, C.K.; Majid, N.I.; Mohd Zainol, M.K.; Mohamad, H.; Mohd Zin, Z. Preliminary Phytochemical Screening and Effect of Hot Water Extraction Conditions on Phenolic Contents and Antioxidant Capacities of *Morinda citrifolia* Leaf. *Malaysian Appl. Biol.* **2018**, *47*, 13–24.
57. Tiwari, S.; Nepal, S.; Sigdel, S.; Bhattarai, S.; Rokaya, R.K.; Pandey, J.; Khadka, R.B.; Aryal, P.; Bhandari, R. Phytochemical Screening, Antibacterial-Guided Fractionation, and Thin-Layer Chromatography Pattern of the Extract Obtained from *Diploknema butyracea*. *Pharmacogn. Res.* **2020**, *12*, 437–443. [CrossRef]
58. Lade, B.D.; Shanware, A.S. Phytonanofabrication: Methodology and Factors Affecting Biosynthesis of Nanoparticles. In *Smart Nanosystems for Biomedicine, Optoelectronics and Catalysis*; Shabatina, T., Vladimir, B., Eds.; IntechOpen: London, UK, 2020; pp. 1–17. ISBN 9781838802547.
59. Adebayo-Tayo, B.; Salaam, A.; Ajibade, A. Green Synthesis of Silver Nanoparticle Using *Oscillatoria* sp. Extract, Its Antibacterial, Antibiofilm Potential and Cytotoxicity Activity. *Heliyon* **2019**, *5*, e02502. [CrossRef]
60. Rai, M.; Ingle, A.; Gupta, I.; Birla, S.; Yadav, A.; Abd-Elsalam, K. Potential Role of Biological Systems in Formation of Nanoparticles: Mechanism of Synthesis and Biomedical Applications. *Curr. Nanosci.* **2013**, *9*, 576–587. [CrossRef]
61. Brand-Williams, W.; Cuvelier, M.E.; Berset, C. Use of a Free Radical Method to Evaluate Antioxidant Activity. *LWT Food Sci. Technol.* **1995**, *28*, 25–30. [CrossRef]
62. Foss, K.; Przybyłowicz, K.E.; Sawicki, T. Antioxidant Activity and Profile of Phenolic Compounds in Selected Herbal Plants. *Plant Foods Hum. Nutr.* **2022**, *77*, 383–389. [CrossRef] [PubMed]
63. Murray, P.R.; Baron, E.J.; Landry, M.L.; Jorgensen, J.H.; Pfallier, M.A. *Manual of Clinical Microbiology*, 9th ed.; American Society for Microbiology: Washington, DC, USA, 2007; Volume 1.
64. Gonelimali, F.D.; Lin, J.; Miao, W.; Xuan, J.; Charles, F.; Chen, M.; Hatab, S.R. Antimicrobial Properties and Mechanism of Action of Some Plant Extracts against Food Pathogens and Spoilage Microorganisms. *Front. Microbiol.* **2018**, *9*, 1639. [CrossRef] [PubMed]